Analytical Methods

A Nuclease Protection ELISA Assay for Colorimetric and Electrochemical Detection of Nucleic Acid

Journal:	*Analytical Methods*
Manuscript ID	AY-ART-12-2018-002729.R1
Article Type:	Paper
Date Submitted by the Author:	22-Jan-2019
Complete List of Authors:	Filer, Jessica; Colorado State University, Microbiology, Immunology, and Pathology Channon, Robert; Imperial College London, Bioengineering Henry, Charles; Colorado State University, Chemistry; Geiss, Brian; Colorado State University, Microbiology, Immunology, and Pathology

Journal Name

ARTICLE

A Nuclease Protection ELISA Assay for Colorimetric and Electrochemical Detection of Nucleic Acid

Jessica E. Filer,[a,b] Robert B. Channon, [c] Charles S. Henry,*[c,d] and Brian J. Geiss *[a,d]

Received 00th January 20xx,
Accepted 00th January 20xx

DOI: 10.1039/x0xx00000x

www.rsc.org/

Early and accurate diagnosis is crucial to monitor infection outcomes and provide timely interventions. However, gold standard polymerase chain reaction assays (PCR) are labor-intensive and require expensive reagents and instrumentation. Nuclease protection has been used for decades to detect and quantify nucleic acid but has not yet been investigated as a diagnostic tool for infectious disease. In this work, we describe a nuclease protection enzyme-linked immunosorbent assay (NP-ELISA) for accurate and sensitive detection of nucleic acid. Briefly, binding of a nucleic acid target to an oligo probe protects it from digestion of un-hybridized nucleic acid by S1 nuclease. Following the workflow of an ELISA, a horseradish peroxidase (HRP)-conjugated antibody binds the probe and oxidizes its substrate to generate signal. The assay was validated with three HRP substrates for absorbance, chemiluminescent, and electrochemical readouts, demonstrating great versatility. Electrochemical detection with 3,3',5,5'-Tetramethylbenzidine (TMB) gave the highest assay sensitivity with a limit of detection of 3.72×10^3 molecules mL^{-1}. Furthermore, non-complementary targets did not generate a response, indicating a high degree of specificity. This proof of principle serves as a stepping stone towards developing miniaturized, multiplexed nuclease protection assays for point-of-care diagnosis.

1. Introduction

Nuclease protection has been an essential tool in molecular biology for over forty years and is an ideal candidate for a simplified nucleic acid detection (NAT) platform. This technique employs an endonuclease such as S1 nuclease [1], mung bean nuclease [2], or RNAse [3] that demonstrates specificity for single-stranded nucleic acids. Traditionally, DNA or RNA that is hybridized to a DNA probe is "protected" from endonuclease digestion and is detected via gel electrophoresis analysis [4]. Nuclease protection assays demonstrate high specificity and are effective alternatives for techniques such as Northern blotting and PCR for NAT [5]. They were first employed in molecular genetics as a technique to map elements of the genome [6] or quantify messenger RNA transcripts [7,8] and their traditional use has been extended to investigate drug immunotoxicity [9] and transgenic expression [10]. Nuclease protection has also been used to detect endogenous [2,11] and viral [5,12] microRNA. More recently, nuclease protection has been integrated with sandwich hybridization assays (SHAs) for colorimetric detection and monitoring of environmental algal species [13–15]. Some research has been directed toward clinical use of nuclease protection to detect biomarkers associated with cancer [16–20] or genetic disorders [21] but to date, no work has been done to investigate its potential as an infectious disease diagnostic.

Many viral diseases including Zika virus, influenza, dengue virus, and chikungunya virus present with general, nonspecific symptoms that encumber differential diagnosis [22]. Thus, the Center for Disease Control (CDC) typically recommends NAT on serum, urine, or other biologically-relevant samples to diagnose viral disease during the early stage of infection [23,24]. This is typically done with approved real-time PCR assays which exhibit good specificity and sensitivity – often with limits of detection around 10^3 genome copy equivalents (GCE) mL^{-1} [25]. However, the real-time PCR assay is very technical, requiring design of three sequence-specific probes in conserved regions of the viral genome with expensive fluorescent and quenching tags [25]. Many diseases like Zika virus are associated with medical complications that necessitate monitoring and timely intervention. While gel-based nuclease protection assays have previously served as an effective alternative for PCR in research [5], the lengthiness and technicality of gel analysis limits the traditional assays use as a diagnostic.

To improve the potential of nuclease protection assays as a clinical diagnostic, gel analysis of nuclease protection can be replaced with enzymatic readout. Cai et al developed a nuclease protection sandwich hybridization assay (NPA-SH) in 2006 with an enzyme-mediated signal output [26]. Although the assay was subsequently used by other groups for environmental monitoring [13,15], the NPA-SH format requires three DNA oligo

[a] Department of Microbiology, Immunology, and Pathology, Colorado State University, Fort Collins, CO 80523, USA
[b] Cell and Molecular Biology Graduate Program, Colorado State University, Fort Collins, CO 80523, USA
[c] Department of Chemistry, Colorado State University, Fort Collins, CO 80523, USA
[d] School of Biomedical Engineering, Colorado State University, Fort Collins, CO 80523, USA
* Corresponding Author
Email Brian.Geiss@colostate.edu, Chuck.Henry@colostate.edu

Electronic Supplementary Information (ESI) available: Electrochemical Characterization of Hydroquinone/Benzoquinone and 3,3',5,5'-Tetramethylbenzidine See DOI: 10.1039/x0xx00000x

probes: a NPA probe, capture probe, and a signal probe. Designing three separate probes for every target of interest increases the assay complexity and limits its adaptability to other potential analytes.

Here, we report a proof-of-principle nuclease protection-ELISA (NP-ELISA) for the specific and sensitive detection of nucleic acid (Figure 1). In contrast to the NPA-SH, the NP-ELISA uses a single oligo capture probe which was designed in this case to have specificity towards a respective Zika (ZIKV) or Kunjin (KUNV) virus sequence. The capture probe is mixed with a nucleic acid target (i) and hybridized products (ii) are immobilized to the bottom of a microtiter plate and are subjected to a digestion reaction with S1 nuclease which degrades single stranded nucleic acid including unbound probe (iii). HRP-conjugated anti-Digoxigenin antibody binds to a digoxigenin molecule bound to the 3' end of the capture probe and facilitates an enzymatic readout (iv). The assay was validated using synthesized target oligos and then compared for colorimetric, chemiluminescent, and electrochemical detection methods. Although electrochemical detection yielded the best sensitivity, the assay is adaptable to all three formats. The NP-ELISA is a new valuable approach for NAT that uses fewer reagents and inexpensive instrumentation compared to real-time PCR.

2. Materials and Methods

2.1 Materials

NP-ELISA assays were performed in clear Neutravidin/BSA treated 8-well strips (ThermoScientific Cat# 15128) for absorbance and electrochemical assays and High Sensitivity Streptavidin black 8 well strips (ThermoScientific, Cat#15525) for chemiluminescence assays. S1 nuclease was purchased from Invitrogen (Cat#EN0321). Ultra TMB-ELISA and SuperSignal ELISA Femto Maximum Sensitivity Substrate were purchased from ThermoScientific (Cat#34028 and Cat#37075). HRP-conjugated anti-Digoxigenin antibody was purchased from AbCam (Cat#ab6212). 5× Hybridization buffer was made with final concentrations of 1.5 M NaCl, 5 mM EDTA, and 190 mM HEPES, pH 7.0 [27]. Digestion buffer (3 M NaCl, 20 mM Zn acetate, and 600 mM Na acetate, pH 4.5) was used for S1 nuclease digestion [27]. Dilution buffer for the nuclease was made according to the manufacturer's protocol. All buffers were made with Millipore Milli-Q water (18 MΩ cm^{-1}), filtered with a 0.45 µm filter membrane, and stored at 4˚ C. Oligonucleotide probe and target sequences specific for a section of the envelope protein coding region in Zika (target/probe 1) and West Nile virus Kunjin subtype (target/probe 2) viruses (Genbank Accession # KU501215 and AY274504, respectively) were synthesized by Integrated DNA Technologies. Sequences were as follows:

BG992 (Probe 1): 5' Biotin-TTTGCACCATCCATCTCAGCCTCC-Digoxigenin

BG993 (Target 1): GGAGGCTGAGATGGATGGTGCAAA

BG975 (Probe 2): 5' Biotin-TAGTATGCACTGGTGTCTATCCCT-Digoxigenin

BG1082 (Target 2): AGGGATAGACACCAGTGCATACTA

BG859 (Extended Target 2):
CAGGGATAGACACCAGTGCATACTATGTGATGACTGTCGG

BG 946 (Scrambled Target 2 nonspecific control):
AGCACGTGTCCGTTGTTATTGGAGTACGCACCGAGAAGAA

BG860 (Target 2 90% complementary target):
CAGCGATAGAGACCAGGGCATACTAAGTGATGACTGTCGG

BG861 (Target 2 80% complementary target):
CAGCGAAAGAGACGAGGGCATACAAAGTGTTGACTGTCGG

2.2 Hybridization and Digestion

A 25 µL solution of 50 fmol probe oligos (BG975 or BG992), 0.5× hybridization buffer, and the indicated target amount were added to a microtube. Probe and target oligos were denatured at 95˚C for 1 minute followed by annealing at 50˚C for 2 minutes. After the annealing step, the hybridized probe:target mixture was transferred to the plate. Prior to use, neutravidin-coated plates were rinsed with 200 µL/well with 1× TBST buffer and incubated for 5 minutes. The digestion reaction mix (final concentrations of 1× S1 digestion buffer and 50U of S1 nuclease) was added to each well and the plate was incubated at 42˚C for 1h. The plate was rinsed five times with 200 µL rinses of 1× TBST and incubated for 5 minutes in between each wash. After rinsing, target detection was performed as described in the following section.

2.3 Absorbance Detection

Absorbance detection was performed in clear 8-well strips using TMB ELISA substrate after the S1 nuclease digestion step. 100 µL of 1:1000 anti-digoxigenin antibody was added to each well and allowed to incubate for one hour at room temperature. After antibody incubation, wells were again washed five times with 1× TBST buffer. 100 µL of UltraTMB-ELISA was added to each well. Plates were incubated for 30 minutes at room temperature and then the HRP reaction was quenched with the addition of 100 µL of 2 M H_2SO_4. Absorbance at 450 nm was measured using a PerkinElmer VICTOR X5 plate reader. Data was analyzed with Prism GraphPad software.

2.4 Chemiluminescence Detection

Chemiluminescence detection was performed in black 8-well strips using a SuperSignal ELISA Fempto Maximum Sensitivity Substrate. After antibody incubation, wells were washed five times with 1× TBST. 100 µL of substrate was added to each well and allowed to incubate for no longer than five minutes. Total luminescence was measured using a PerkinElmer VICTOR X5 plate reader. Data was analyzed with Prism GraphPad software.

2.5 Electrochemical Detection

Electrochemical assays were performed in clear 8-well strips using a CHI1242B Potentiostat (CH Instruments, Inc, TX). A 25 µm diameter Au disk microelectrode (CH Instruments, Model CHI106) was used as the working electrode. The working electrode was polished with an alumina slurry (0.1 µm diameter), washed with water, then cleaned electrochemically through cycling in 50mM KOH before each use. An Ag/AgCl microelectrode (25µm diameter, eDAQ, Colorado Springs) was used as the reference/counter electrode in a

two-electrode setup. After the rinses, 100µL of 1:1000 anti-digoxigenin was added to each well and incubated for 1 hour at room temperature. After antibody incubation, wells were again washed five times with 1× TBST buffer. 100 µL of Ultra TMB-ELISA or 100 µL of 1mM hydroquinone (HQ) with 0.1% H_2O_2 were added to each well and incubated for 30 minutes. The oxidation of TMB or HQ was quenched with 10 µL of 8 M H_2SO_4. SWV measurements were taken in a range of -0.2 V to 1.4 V for TMB and 0.4 V to -0.4 V for HQ at a frequency of 15 Hz and were conducted in a CS-3A Cell Stand faradaic cage. SWV curves were averaged and the peaks were integrated from ~0.47 V to ~0.62 V using the automatic peak finding function of the CHI1242B software. The data was then analyzed with Prism GraphPad software.

3. Results and Discussion

3.1 Optimization of Nuclease Protection

Oligo probes were designed with sequence specificity for either ZIKV (Target 1; BG992) or KUNV (Target 2; BG975). To optimize the probe concentration for use in the assay, BG992 and BG975 were titrated out and incubated with anti-digoxigenin HRP-conjugated antibody. The signal response was analyzed with absorbance and the results are presented in Figure 2a. As expected, increasing concentrations of probe increased the signal response until the signal saturated at 6×10^{12} molecules mL^{-1}. Similar results were obtained for both the ZIKV and the KUNV probes, suggesting that oligo sequence should not affect the detection mechanism. A dynamic range of 6×10^{10} - 6×10^{12} molecules mL^{-1} was determined, spanning three orders of magnitude. The probe concentration that gave the highest signal without saturation was 6×10^{12} molecules mL^{-1} and was used for downstream applications.

The effect of S1 nuclease concentration on the absorbance signal was also investigated (Figure 2b). The enzyme was serially diluted and allowed to catalyze degradation of 6×10^{12} molecules mL^{-1} (50 fmol) of probe (BG992) bound to the neutravidin plate in S1 digestion buffer for 1 hour at 42˚ C. Maximum signal was retained with increasing amounts of nuclease from 5 µU to 0.5 U. Addition of 5 U of nuclease caused the signal to drop dramatically and 50U resulted in a complete loss of signal. To ensure complete degradation and removal of unbound nucleic acid, 50 U (5 µL of 10 U/µL) of nuclease was chosen for further experiments.

DNA oligo targets (Target 1 (BG993) or Target 2 (BG1082)) and complementary probes (Probe 1 (BG992) or Probe 2 (BG975)) were designed and synthesized to test target detection by nuclease protection. The targets were hybridized to their respective probe and unbound probe was digested with S1 nuclease. A range of concentrations were then tested to determine the linear dynamic range (LDR) and the limit of detection (LOD). For the absorbance readout, 3,3',5,5'-Tetramethylbenzidine (TMB) was used as a colorimetric substrate for HRP. The results in Figure 3a demonstrate a sigmoidal response with a linear dynamic range of 9.64×10^{10} – 1.20×10^{13} molecules mL^{-1}. This range is consistent with that obtained for the probe titration. LOD is generally calculated using the linear calibration curve according to ICH standard [28], through

$$\mathbf{LOD} = \frac{\mathbf{3.3}\sigma}{S} \quad (1)$$

where σ is the standard deviation of the y-intercept and S is the slope of the regression line. We found, however, that using this method for absorbance detection produced artificially low LODs that did not account for the signal drop-off outside the dynamic range. The LOD was instead calculated via

$$\mathbf{LOD} = \boldsymbol{\mu}_{\mathbf{blank}} + \mathbf{3}\boldsymbol{\sigma}_{\mathbf{blank}} \quad (2)$$

where μ_{blank} and σ_{blank} are the mean and standard deviation respectively of a series of blank samples [29]. With this method (equation 2), the LOD was calculated to be 9.80×10^{10} molecules mL^{-1}. To place our results in perspective, the CDC reported an LOD of 2.45×10^{3} genome copy equivalents (GCE) mL^{-1} for their Trioplex real time PCR assay which is used to detect ZIKV, dengue virus, and chikungunya virus [25]. Because the LOD for the absorbance readout is several orders higher than comparable clinical assays, it may limit the absorbance assay's applicability to viral diagnostics. However, the absorbance NP-ELISA may still be used for accurate detection of nucleic acid at higher concentrations.

3.2 NP-ELISA Specificity

To test the specificity of the NP-ELISA, nuclease protection was attempted with nonspecific target oligos. As shown in Figure 3a, when increasing amounts of Target 2 (BG1082) are added to Probe 1 (BG992), no protection was observed. Likewise, when Target 1 (BG993) was added to the Probe 2 (BG975), no protection was observed. This indicates that the nonspecific target is not able to protect the probe and thus the probe oligos are digested by the enzyme in the presence of non-specific targets. To further validate the specificity of the assay, three different nonspecific targets were employed. The targets were scrambled to have 90% (36/40 matched base pairs), 80% (32/40) or 0% complementarity to Probe 2 while maintaining equivalent GC%. They were added to the reaction in 5× excess compared to the probe concentration. The results (Figure 4) show that even with high sequence similarity (4 mismatches or 8 mismatches, 90% and 80% complementarity respectively), nonspecific targets provide virtually no protection to the probe oligo from S1 nuclease digestion and do not differ significantly from the negative control (no probe). These data suggest a high specificity that may be further confirmed by testing protection with 1-3 mismatches and agree with the reported use of nuclease protection to detect single nucleotide mutations [30–32]. The targets for the specificity assay, including the 100% complementary oligo, were designed to have overhanging sequences. These data also suggest that overhanging target DNA sequences do not have a significant effect on specific target detection.

3.3 Increasing NP-ELISA Sensitivity through Chemiluminescent and Electrochemical Detection

Because the LOD for NP-ELISA absorbance detection is significantly higher than LODs for clinically used assays like the Trioplex assay [25], chemiluminescent and electrochemical HRP detection schemes

were tested to see if the LOD could be significantly improved. Chemiluminescent substrates have been used in place of colorimetric substrates to increase the sensitivity of ELISAs [33]. The assay was tested with SuperSignal ELISA Fempto Maximum Sensitivity Substrate for detection (Figure 3b), which yielded a comparable, though slightly smaller dynamic range compared to absorbance (4.82×10^{11} – 1.20×10^{13} molecules mL^{-1}). Because the chemiluminescent substrate did not significantly increase assay sensitivity, no further experiments were performed with the chemiluminescent substrate.

HRP oxidizes TMB in a two-step irreversible process. The first one-electron oxidation of TMB produces a blue-colored product consisting of an equilibrium between the cation free-radical and a charge transfer complex of the precursor diamine and its diimine oxidation product [34,35]. At acidic pHs, the second-electron oxidation product becomes stable, yielding the yellow-colored diamine [34,36]. These two products can be quantified with absorbance at 370nm and 420nm respectively [34]. TMB and its oxidized forms are also electrochemically active, generating a faradaic current that can be detected by electrochemical techniques. The concept of a plate-based electrochemical immunoassay was published as early as the 1980s [37], but has not been widely studied and has been overshadowed by immunosensor research. Electrochemical detection typically provides lower LODs, wider dynamic ranges, and better sensitivity compared to absorbance techniques [38]. Additionally, interference from turbid or colored samples is not an issue for electrochemical analysis as it is the case spectrophotometric techniques [39]. Lastly, the instrumentation for voltammetry is relatively inexpensive (~$2000 USD) when compared to a real time PCR system (~$15,000 USD) or even a plate reader (~$5000 USD) and is easily miniaturized [39].

To see if electrochemistry could increase the NP-ELISA assay's sensitivity, TMB and hydroquinone were characterized with cyclic voltammetry as electrochemical HRP substrates and optimized for square wave voltammetry detection (Supplementary Information Figures S1-S4). Square wave voltammetry (SWV) is a pulsed technique known to be both fast and highly sensitive [40]. As a differential method, the peak height of a SWV curve is not always proportional to the concentration of the species, so peak area integration was employed to give a more accurate readings [41]. Although TMB is an easily accessible reagent for electrochemical detection, some research has shown an inability to detect TMB using SWV [42]. Hydroquinone (HQ) was tested and compared to TMB as another electroactive substrate for HRP that has been effectively used in biosensor platforms [43–45]. TMB and HQ were compared in the NP-ELISA for sensitivity and the results are shown in Figure 5. A probe titration was performed for electrochemical detection with both TMB and HQ to optimize the probe amount for the electrochemical assay. HQ as a substrate yielded a wider dynamic range (6.02×10^5 – 6.02×10^{15} molecules mL^{-1}) compared to the absorbance readout with TMB, but the variability was higher (Figure 5d). The probe titration data for TMB (Figure 5b) shows a dynamic range of 0 – 6×10^{11} molecules mL^{-1}, which is several magnitudes larger than the absorbance readout (9.64×10^{10} – 1.20×10^{13} molecules mL^{-1}), suggesting a much higher sensitivity for electrochemical TMB readout versus absorbance readout. At concentrations greater than 6×10^{13} molecules mL^{-1}, the oxidized TMB rapidly precipitates out of solution and yields little to no electrochemical signal. However, in the tested range, TMB peaks were sharper and more defined than the HQ peaks (Figure 5a and 5c respectively). Given its demonstrated superiority as an electrochemical substrate, TMB was chosen over HQ for downstream applications. A probe concentration of 6×10^{12} molecules mL^{-1} (50 fmol) was chosen for electrochemical target detection.

3.4 Sensitivity of Electrochemical Detection

The sensitivity of the NP-ELISA with TMB-based electrochemical detection was assessed for a DNA oligo target (Figure 6). A dynamic range of 0 - 6×10^{13} molecules mL^{-1} was determined, in agreement with the electrochemical probe titration. While electrochemical detection has a significantly higher sensitivity than absorbance, poor reproducibility at low concentrations may limit the accuracy of the assay. Reproducibility may be improved by using electroactive substrates that mitigate the quasi-reversibility of the TMB reaction and the fouling of the electrode with electrochemical species. The LOD was calculated using the calibration line according to the ICH guidelines [28] via Equation 1. The LOD was determined to be 3.72×10^3 molecules mL^{-1}. Reported viral loads range from 10^3-10^8 GCE mL^{-1} in blood and urine [46]. The dynamic range for the NP-ELISA is significantly wider than the reported clinical range and the calculated LOD is similar to that of the Trioplex assay at 2.45×10^3 GCE mL^{-1} [25]. By detecting such small amounts of nucleic acid, clinicians may be able to diagnose infection sooner and enable earlier medical intervention for at-risk fetuses.

4. Conclusion

In this work, we have described a novel nuclease protection ELISA (NP-ELISA) that has clinical relevance as an alternative to real time RT-PCR. The assay has excellent specificity with highly similar sequences and is compatible with multiple signal visualization modalities. Electrochemical detection can reach an LOD of 3.72×10^3 molecules mL^{-1}, within a relevant clinical range for nucleic acid detection. Further research is required to address the limitations of this study. Because a synthetic system was used to assess proof-of-concept principles, more work is required to address the functionality of the assay with biological samples. Furthermore, poor reproducibility at low concentrations can obscure the accuracy of electrochemical analysis and may be a result of the quasi-reversible nature of these redox reactions and the propensity of these species to foul the electrode surface (described in Supplementary Information). However, potentiostats for electrochemical detection are significantly less expensive and more portable than real time PCR systems, making the assay more accessible for sensing or screening in remote areas. Our previous research with microwire electrodes shows that electrochemical detection is easily miniaturized into handheld, disposable paper sensors [47,48] and our research group is

currently working to implement the NP-ELISA on microwires for antibody-less, hand-held detection of nucleic acids.

In addition to its capacity for miniaturization, the NP-ELISA has large potential as a multiplexed assay. For the antibody-based assay, sequence specific probes can be designed with conjugated small molecules other than digoxigenin. Antibodies specific for these small molecules can be conjugated to different enzymes with different electroactive substrates. Because oxidation or reduction of the reaction products would occur at different potentials, one potential sweep would allow the user to identify each target in a single sample at a different potential. This greatly increases the NP-ELISA's usefulness as a differential diagnostic tool. The data presented here as well as above mentioned future directions suggest that the NP-ELISA is a viable alternative for clinical NAT with potential for direct, multiplexed, and hand-held detection of pathogen nucleic acids.

Conflicts of interest

We have no conflicts to declare.

Acknowledgements

The authors would like to thank Joe Russo, Erin Lynch, and Kristen Bullard-Feibelman for technical assistance. We also would like to thank the members of the Geiss, Wilusz, and Henry laboratories for helpful comments and discussion. This work was partially supported by a National Science Foundation grant (DGE-1450032). Any opinions, findings, conclusions, or recommendations expressed are those of the authors and do not necessarily reflect the views of the National Science Foundation. This work was also supported by the National Institute of Health [5 R01 AI114675 and 1 R01 AI132668] to BJG and Colorado State University to RBC and CSH.

References

1. E. Eyler, in *Methods in Enzymology*, Elsevier Inc., 1st edn., 2013, vol. 530, pp. 89–97.
2. S.-Y. Hou, Y.-L. Hsiao, M.-S. Lin, C.-C. Yen, and C.-S. Chang, *Talanta*, 2012, **99**, 375–379.
3. R. A. Roberts, C. M. Sabalos, M. L. LeBlanc, R. R. Martel, Y. M. Frutiger, J. M. Unger, I. W. Botros, M. P. Rounseville, B. E. Seligmann, T. P. Miller, T. M. Grogan, and L. M. Rimsza, *Lab. Investig.*, 2007, **87**, 979–997.
4. D. R. Smith, in *Transgenesis Techniques*, Humana Press, New Jersey, 1993, vol. 18, pp. 363–372.
5. M. John and S. Pfeffer, in *Methods in molecular biology (Clifton, N.J.)*, 2011, vol. 721, pp. 173–182.
6. F. M. Cammas and A. J. L. Clark, *Anal. Biochem.*, 1996, **236**, 182–184.
7. A. J. Berk and P. A. Sharp, *Cell*, 1977, **12**, 721–732.
8. M. Goldrick and D. Kessler, in *Current Protocols in Neuroscience*, John Wiley & Sons, Inc., Hoboken, NJ, USA, 2003.
9. R. N. Fichorova, K. Mendonca, H. S. Yamamoto, R. Murray, N. Chandra, and G. F. Doncel, *Toxicol. Appl. Pharmacol.*, 2015, **285**, 198–206.
10. M. H. Irwin and C. A. Pinkert, in *Transgenic Animal Technology*, Elsevier, 2014, pp. 543–564.
11. M. John, R. Constien, A. Akinc, M. Goldberg, Y. Moon, M. Spranger, P. Hadwiger, J. Soutschek, H. Vornlocher, M. Manoharan, M. Stoffel, R. Langer, D. G. Anderson, J. D. Horton, V. Koteliansky, and D. Bumcrot, *Nature*, 2007, **449**, 745–747.
12. L. Dolken, J. Perot, V. Cognat, A. Alioua, M. John, J. Soutschek, Z. Ruzsics, U. Koszinowski, O. Voinnet, and S. Pfeffer, *J. Virol.*, 2007, **81**, 13771–13782.
13. Y. Zhen, T. Mi, and Z. Yu, *Harmful Algae*, 2009, **8**, 651–657.
14. X. Zhu, Y. Zhen, T. Mi, and Z. Yu, *Mar. Biotechnol.*, 2012, **14**, 502–511.
15. S.-S. Suh, M. Park, J. Hwang, E.-J. Kil, S. Lee, and T.-K. Lee, *Biotechnol. Lett.*, 2016, **38**, 57–63.
16. B. Tanner, T. Friedberg, M. Mitze, T. Beck, F. Oesch, and P.-G. Knapstein, *Gynecol. Oncol.*, 1992, **47**, 228–233.
17. L. Sun and J. Irudayaraj, *J. Phys. Chem. B*, 2009, **113**, 14021–14025.
18. D. Bose, G. Jayaraj, H. Suryawanshi, P. Agarwala, S. K. Pore, R. Banerjee, and S. Maiti, *Angew. Chemie Int. Ed.*, 2012, **51**, 1019–1023.
19. B. Pilato, S. De Summa, K. Danza, S. Papadimitriou, P. Zaccagna, A. Paradiso, and S. Tommasi, *Mol. Biotechnol.*, 2012, **52**, 8–15.
20. B. K. Thakur, H. Zhang, A. Becker, I. Matei, Y. Huang, B. Costa-Silva, Y. Zheng, A. Hoshino, H. Brazier, J. Xiang, C. Williams, R. Rodriguez-Barrueco, J. M. Silva, W. Zhang, S. Hearn, O. Elemento, N. Paknejad, K. Manova-Todorova, K. Welte, J. Bromberg, H. Peinado, and D. Lyden, *Cell Res.*, 2014, **24**, 766–769.
21. S. Bannwarth, V. Procaccio, and V. Paquis-Flucklinger, *Hum. Mutat.*, 2005, **25**, 575–582.
22. M. Goeijenbier, L. Slobbe, A. van der Eijk, M. de Mendonça Melo, M. P. G. Koopmans, and C. B. E. M. Reusken, *Neth. J. Med.*, 2016, **74**, 104–9.
23. Centers for Disease Control and Prevention, 2017.
24. Centers for Disease Control and Prevention, 2017.
25. Centers for Disease Control and Prevention, *Trioplex Real-Time RT-PCR Assay Instructions for Use*, 2017.
26. Q. Cai, R. Li, Y. Zhen, T. Mi, and Z. Yu, *Harmful Algae*, 2006, **5**, 300–309.
27. J. Zhou, J. J. Rossi, and R. P. V. R. (Ed.), *Antiviral RNAi*, Humana Press, Totowa, NJ, 2011, vol. 721.
28. ICH Experiment Working Group, in *International Conference on Harmonization*, 2005.
29. J. N. Miller and J. C. Miller, *Statistics and Chemometrics for Analytical Chemistry*, Pearson Education Limited, 6th edn., 2010.
30. C. a Oleykowski, C. R. Bronson Mullins, a K. Godwin, and a T. Yeung, *Nucleic Acids Res.*, 1998, **26**, 4597–4602.
31. B. J. Till, *Nucleic Acids Res.*, 2004, **32**, 2632–2641.
32. Z. Tadele, *Curr. Genomics*, 2016, **17**, 499–508.
33. L. Holec-Gąsior, B. Ferra, J. Czechowska, I. E. Serdiuk, and

K. Krzymiński, *Diagn. Microbiol. Infect. Dis.*, 2018, **91**, 13–19.
34. N. Muhammad, T. Dworeck, M. Fioroni, and U. Schwaneberg, *J. Nanobiotechnology*, 2011, **9**, 8.
35. L. S. A. Busa, T. Komatsu, S. Mohammadi, M. Maeki, A. Ishida, H. Tani, and M. Tokeshi, *Anal. Sci.*, 2016, **32**, 815–818.
36. P. D. Josephy, T. Eling, and R. P. Mason, *J. Biol. Chem.*, 1982, **257**, 3669–75.
37. W. R. Heineman and H. B. Halsall, *Anal. Chem.*, 1985, **57**, 1321A–1331A.
38. H. Sha, Y. Bai, S. Li, X. Wang, and Y. Yin, *Am. J. Orthod. Dentofac. Orthop.*, 2014, **145**, 36–40.
39. F. D. Martínez-Mancera, P. García-López, and J. L. Hernández-López, *Clin. Chim. Acta*, 2015, **444**, 199–205.
40. J. G. Osteryoung and R. A. Osteryoung, *Anal. Chem.*, 1985, **57**, 101A–110A.
41. P. M. S. Monk, *Fundamentals of Electro-Analytical Chemistry*, John Wiley & Sons, Inc., 2008.
42. S. V. Kergaravat, M. I. Pividori, and S. R. Hernandez, *Talanta*, 2012, **88**, 468–476.
43. E. Sánchez-Tirado, G. Martínez-García, A. González-Cortés, P. Yáñez-Sedeño, and J. M. Pingarrón, *Biosens. Bioelectron.*, 2016, 1–6.
44. N. Krithiga, K. B. Viswanath, V. S. Vasantha, and A. Jayachitra, *Biosens. Bioelectron.*, 2016, **79**, 121–129.
45. S. Patris, M. Vandeput, G. M. Kenfack, D. Mertens, B. Dejaegher, and J.-M. Kauffmann, *Biosens. Bioelectron.*, 2016, **77**, 457–463.
46. D. Musso and D. J. Gubler, *Clin. Microbiol. Rev.*, 2016, **29**, 487–524.
47. J. A. Adkins and C. S. Henry, *Anal. Chim. Acta*, 2015, **891**, 247–254.
48. R. B. Channon, Y. Yang, K. M. Feibelman, B. J. Geiss, D. S. Dandy, and C. S. Henry, *Anal. Chem.*, 2018, **90**, 7777–7783.

Journal Name

ARTICLE

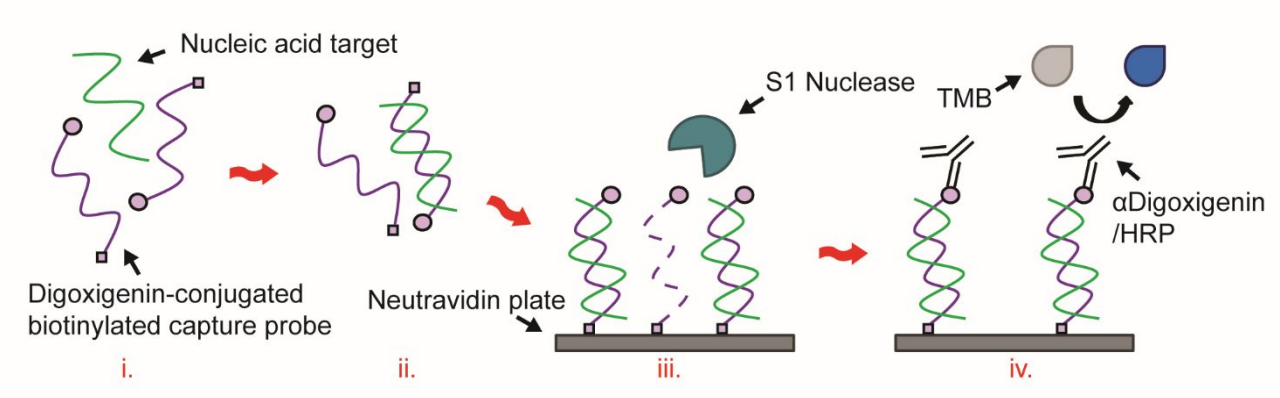

Figure 1. Conceptualization of NP-ELISA. Oligo capture probes specific for ZIKV (BG992) or KUNV (BG975) are mixed with target nucleic acid (i) and are allowed to hybridize (ii). The hybridized probe is immobilized to a neutravidin plate via a 5' biotin molecule (iii). S1 nuclease degrades any unbound probe, leaving only the hybridized probe behind (iii). An HRP-conjugated antibody binds to the 3' Digoxigenin molecule on the probe and catalyzes the oxidation of TMB to produce a colorimetric or electrochemical signal (iv).

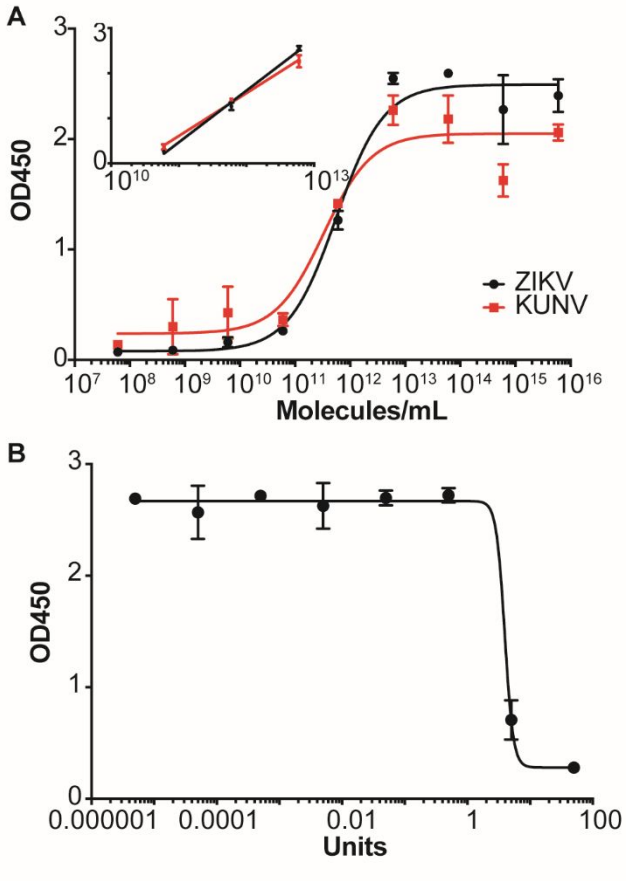

Figure 2. Optimization of nuclease protection. A) The effect of probe concentration on absorbance signal was examined. A sigmoidal response was observed with a dynamic range of 6×10^{10}- 6×10^{12} molecules mL^{-1}. Probe sequence (BG992 vs BG975) had no effect on signal response. Inset shows the linearity of the dynamic range from the sigmoidal response. B) The effect of S1 nuclease concentration on absorbance signal was investigated. Dilutions lower than 5U had no effect on the signal. 50U of enzyme caused total loss of signal, indicating complete digestion of the probe (BG992).

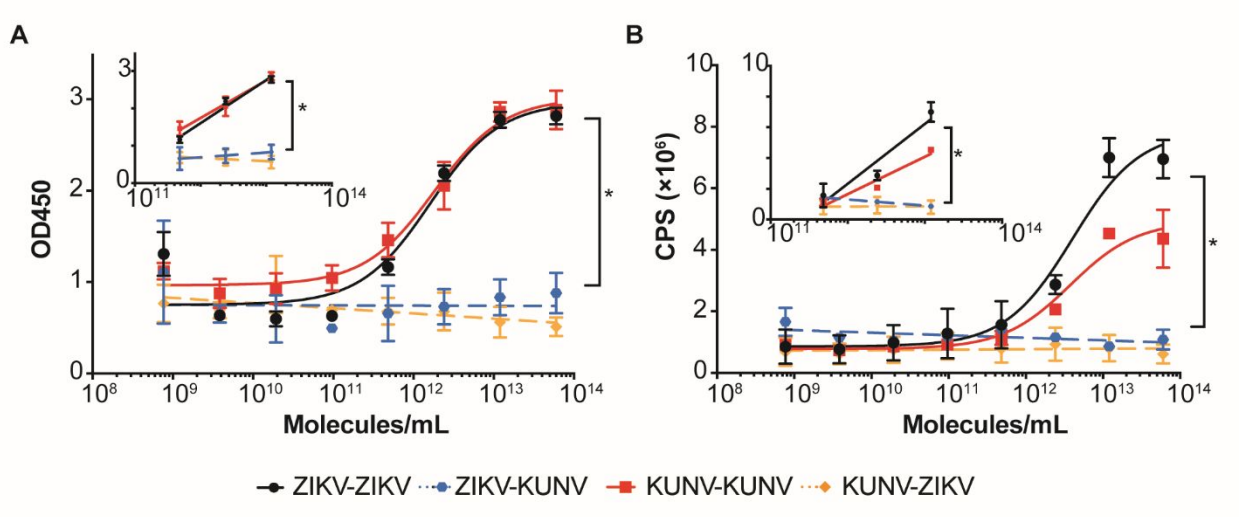

Figure 3. Spectrophotometric Detection of Oligo Target. A) Oligo target was titrated out to determine the effect of target concentration on absorbance signal. A sigmoidal signal response was obtained with a linear dynamic range of $9.64\times10^{10} – 1.20\times10^{13}$ molecules mL^{-1} as shown in the inset. The limit of detection was determined to be 9.80×10^{10} molecules mL^{-1} for absorbance detection. B) A chemiluminescent substrate was used in attempt to increase the sensitivity of spectrophotometric detection. A linear range, shown in the inset, of was determined to be $4.82\times10^{11} – 1.20\times10^{13}$ molecules mL^{-1}, which is smaller than the range determined for absorbance detection. Because chemiluminescent detection did not increase sensitivity, no further experiments were done with the substrate.

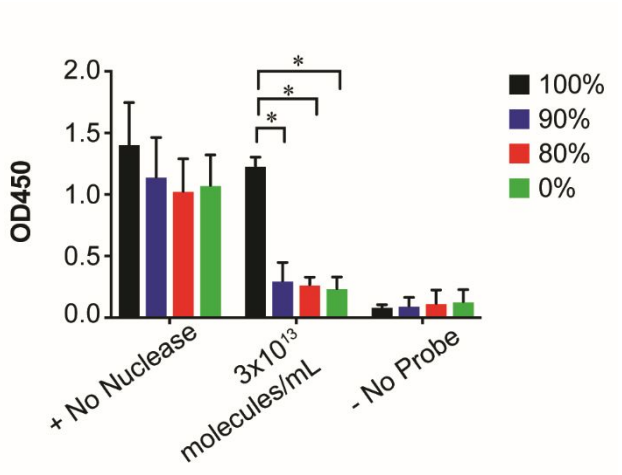

Figure 4. Effect of mutations and target length on nuclease protection. Mutations were added to the target oligos (BG860, BG861, BG946) and tested for capacity for nuclease protection. Even with high complementarity, the signal from mutated targets did not differ significantly from the - control. To test the effect of length on

protection, these targets were designed to have overhanging sequences. Signal from the 100% complementary target (BG859) did not differ significantly from the + control, suggesting that overhangs to not detrimentally affect protection.

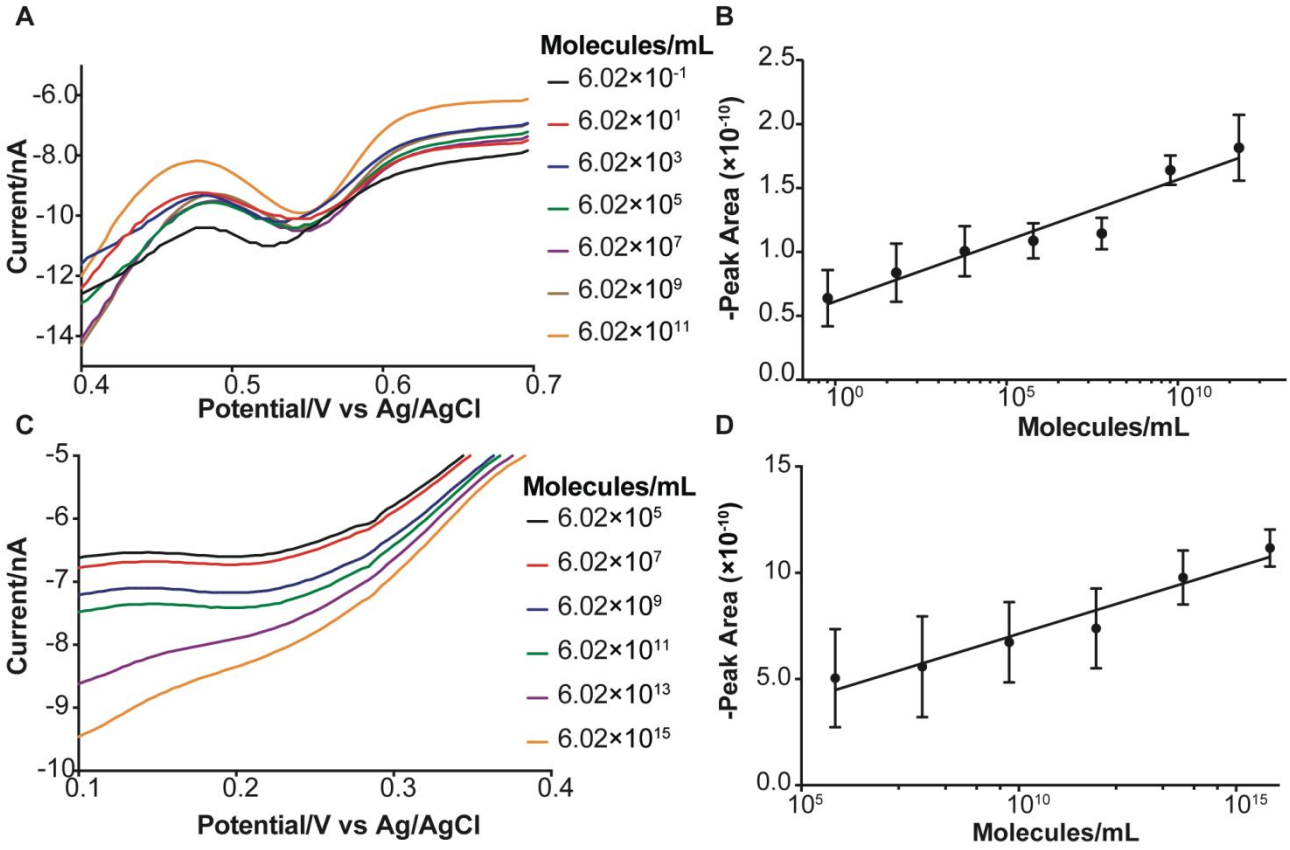

Figure 5. Optimization of Electrochemical Detection. A) Square wave voltammetry results evaluating TMB as an electrochemical substrate for HRP. B) Peaks were integrated and the peak area was plotted against the log of the concentration and a dynamic range of 0 – 6×10^{11} molecules mL^{-1} was determined. C) Square wave voltammetry results for hydroquinone as an alternative substrate for electrochemical detection. D) Peak integration was performed and peak areas were plotted against the log of the concentration. A dynamic range of 6.02×10^{5} – 6.02×10^{15} molecules mL^{-1} was obtained.

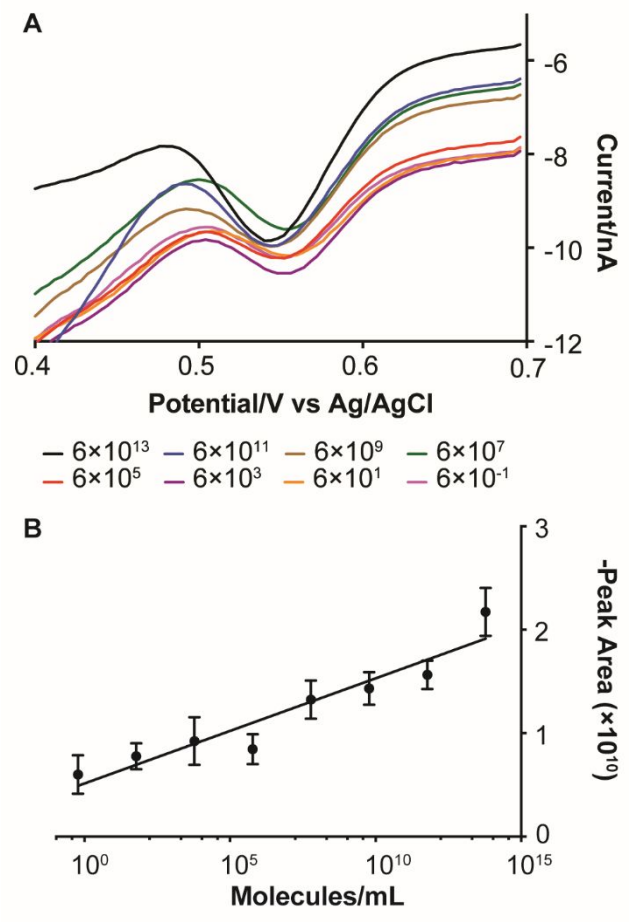

Figure 6. Electrochemical Detection of Target Oligo. A) Square wave voltammetry was used for oligo target detection (BG993). B) The peak area was obtained from 0.45 V to 0.65 V and plotted against the log molecules mL^{-1}. A linear curve of the log-transformed concentration was obtained from 0 - 6×10^{13} molecules mL^{-1} with an LOD of 3.72×10^{3} molecules mL^{-1}.

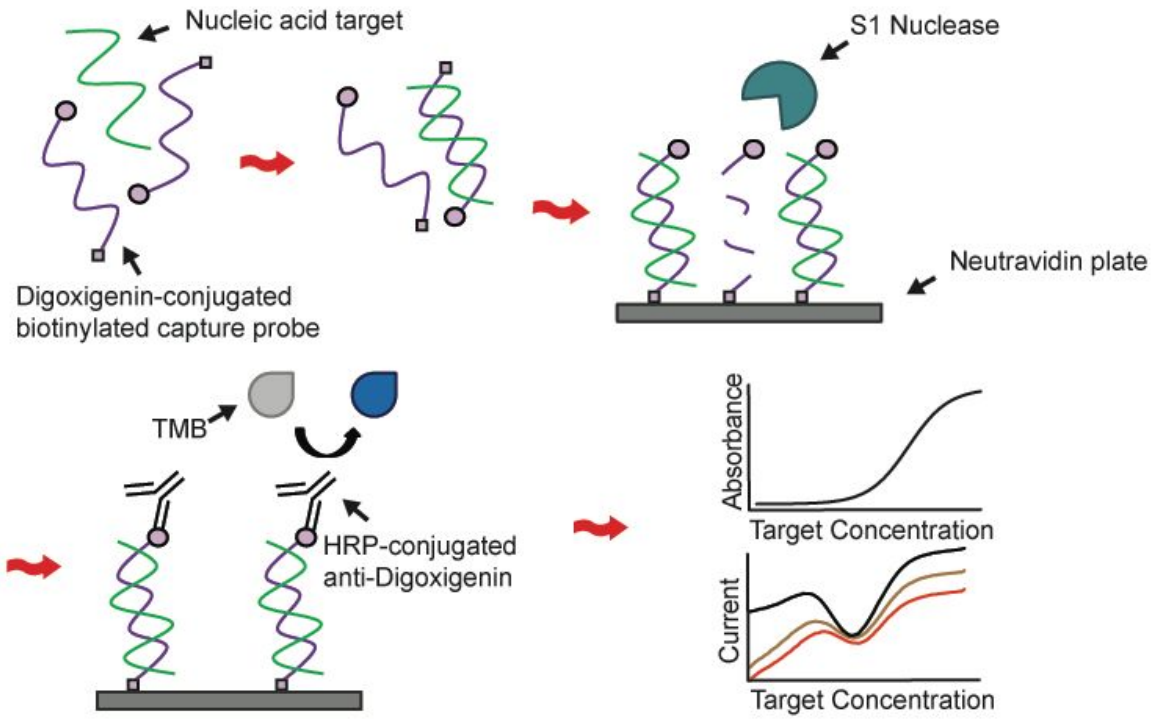

Graphical Abstract

The NP-ELISA combines traditional nuclease protection with optical and electrochemical enzymatic readout for nucleic acid detection.